The Near-Infrared Radiation Received by Satellites from Clouds

G. J. BELL[1] AND M. C. WONG

Royal Observatory, Hong Kong

(Manuscript received 30 October 1980, in final form 2 April 1981)

ABSTRACT

On satellite images in the near-infrared 3.7 μm atmospheric window some low clouds appear warmer than the sea. A simple analysis of the radiation balance of elements of the cloud and sea surface indicates that the anomaly can be explained by the difference in reflectance between these elements. In some areas of the image, low clouds return more reflected solar radiation to the satellite than does the background sea. These clouds may then appear warmer. A method to measure the albedo of clouds using these satellite data is suggested.

1. Introduction

Usually, infrared images from meteorological satellites show bodies with temperatures appropriate to cloud tops in various shades of white—colder being whiter. However, in some images from the Tiros N 3.7 μm near-infrared band some clouds appear dark and; in particular, darker than the sea surface. This is illustrated in Fig. 1 which is an image of the South China Sea area, centered near 16°N, 115°E and received from Tiros N at 0725 GMT on 26 April 1979 via the AVHRR channel 3 in the band 3.55–3.93 μm. The clouds to the west of North Luzon appear white on both the visible and 10 μm infrared image shown in Fig. 2 but, in the 3.7 μm near-infrared image these clouds appear dark and, in particular, darker than the sea. At first sight this suggests that the cloud tops are warmer than the sea surface but, such a conclusion is contrary to the indications of both the 10 μm image (Fig. 2) and the synoptic situation. The following simple analysis of the radiation balance involved provides an explanation for this apparent anomaly.

2. Analysis of the radiation balance within the 3.7 μm atmospheric window

The total radiation within the satellite's passband $\Delta\lambda$ reaching the satellite sensor from the element of interest, whether cloud or sea, which fills the field of view of the radiometer is the sum of (i) the net flux radiated by the element, (ii) the flux radiated by the atmospheric molecules and aerosols within the solid angle subtended by the element and *(iii)* the solar flux reflected by the element. Atmospheric attenuation will be neglected as transmission is through the atmospheric window. The contribution from atmospheric aerosols also will be neglected.

The intensity I_e of radiation emitted from an element in the earth's surface is regarded as a function of the latitude, longitude and the zenith angle as well as the azimuthal angle of the exiting ray. If we further approximate the cloud and sea elements to grey surfaces with equivalent temperatures T_c and T_s and emissivities ϵ_c and ϵ_s, then

$$I_{e,c} = \pi^{-1}\epsilon_c B(T_c), \tag{1a}$$

$$I_{e,s} = \pi^{-1}\epsilon_s B(T_s). \tag{1b}$$

In the above equations, $I_{e,c}$, $I_{e,s}$ are the intensity of emitted radiation incident on the sensor from cloud and sea elements, respectively, while $B(T_c)$, $B(T_s)$ are the blackbody radiation values within the band at the temperatures T_c and T_s, respectively. The factor of π^{-1} is the normalization constant.

Formulation of the intensity $I_{r,c}$ of reflected radiation from a cloud element has to take into consideration the sun as a radiation source.

$I_{r,c}$ is a function of the colatitude, longitude, the solar zenith angle (θ), the zenith angle of the reflected ray (ϕ) and the azimuth (ξ) of the reflected ray relative to the sun. It can be expressed in terms of the bidirectional reflectance function $R(\theta, \phi, \xi)$ which is defined as

$$I_{r,c} = B(T_{\text{sun}})\alpha_c(\theta)R(\theta, \phi, \xi). \tag{2a}$$

A similar equation holds for the reflected intensity from a sea element

$$I_{r,s} = B(T_{\text{sun}})\alpha_s(\theta)R(\theta, \phi, \xi), \tag{2b}$$

[1] Deceased.

0027-0644/81/102158-06$05.50

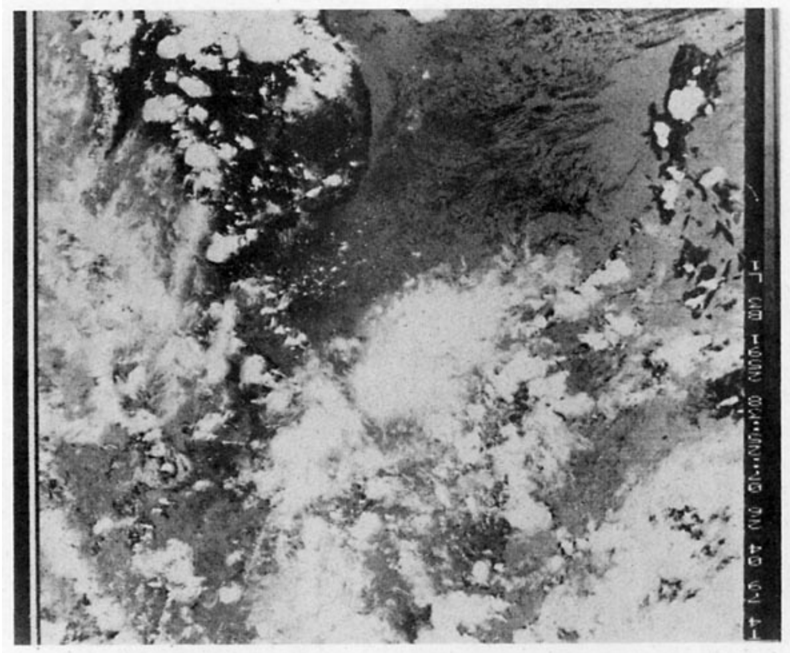

FIG. 1. AVHRR Tiros N image observed through the 3.7 μm atmospheric window over the South China Sea. The clouds of interest appear at top center and the solar specular reflection from the sea is at mid left.

where $B(T_{\text{sun}})$ is the blackbody radiation value within the band at the sun's equivalent temperature $T_{\text{sun}} = 5800$ K, while α_c, α_s are the albedo of the cloud and sea element, respectively, and are assumed to vary with the solar zenith angle only. The bidirectional reflectance function has been assumed to vary only with the solar zenith angle (θ), the zenith of the reflected ray (ϕ) and the azimuth (ξ) between the two and does not vary with reflecting surface. An empirical bidirectional reflectance function $\rho(\theta, \phi, \xi)$ has been modeled by Green (1980) based on Nimbus 3 data. Some values of his modeled function are shown in Table 1.

We model the bidirectional reflectance functions $R(\theta, \phi, \xi)$ as a composite of the Green's empirical model and a diffuse model. We represent $R(\theta, \phi, \xi)$ by a linear combination of the two models, through a parameter $L(0 \leqslant L \leqslant 1)$ as follows:

$$R(\theta, \phi, \xi) = L\rho(\theta, \phi, \xi) + (1 - L)\pi^{-1}. \quad (3)$$

The total intensity of radiation incident on the satellite sensor from the cloud and sea element, I_c and I_s, respectively, is given by

$$I_c = I_{e,c} + I_{r,c}, \quad (4a)$$

$$I_s = I_{e,s} + I_{r,s}. \quad (4b)$$

When the sensor receives more radiation from the cloud element than from the sea, the cloud will appear darker than the sea using the normal display convention. On the satellite image the relative shades of these elements depend on the inequality

$$I_c \gtreqless I_s. \quad (5)$$

If we assume that Kirchoff's law holds within the band, i.e.,

$$\alpha_c + \epsilon_c = 1, \quad (6a)$$

$$\alpha_s + \epsilon_s = 1, \quad (6b)$$

then (5) can be written as

$$G \gtreqless 1,$$

where

$$G = \frac{\pi R(\theta, \phi, \xi)(\alpha_c - \alpha_s)B(T_{\text{sun}})}{(1 - \alpha_s)B(T_s) - (1 - \alpha_c)B(T_c)}. \quad (7)$$

when $G > 1$, the cloud element will appear darker than the sea and vice versa.

Let $P_\lambda(T)$ be the Planck's function at temperature T such that

$$P_\lambda(T) = C_1\lambda^{-5}\left[\exp\left(\frac{C_2}{\lambda T}\right) - 1\right]^{-1}, \quad (8)$$

with

$$C_1 = 3.7403 \times 10^{-16} \text{ W m}^{-2},$$

$$C_2 = 1.4387 \times 10^{-2} \text{ m K}^{-1},$$

If we now define $S(\lambda, T)$ as

$$S(\lambda, T) = \int_0^\lambda P_\lambda(T)d\lambda \Big/ \int_0^\infty P_\lambda(T)d\lambda, \quad (9)$$

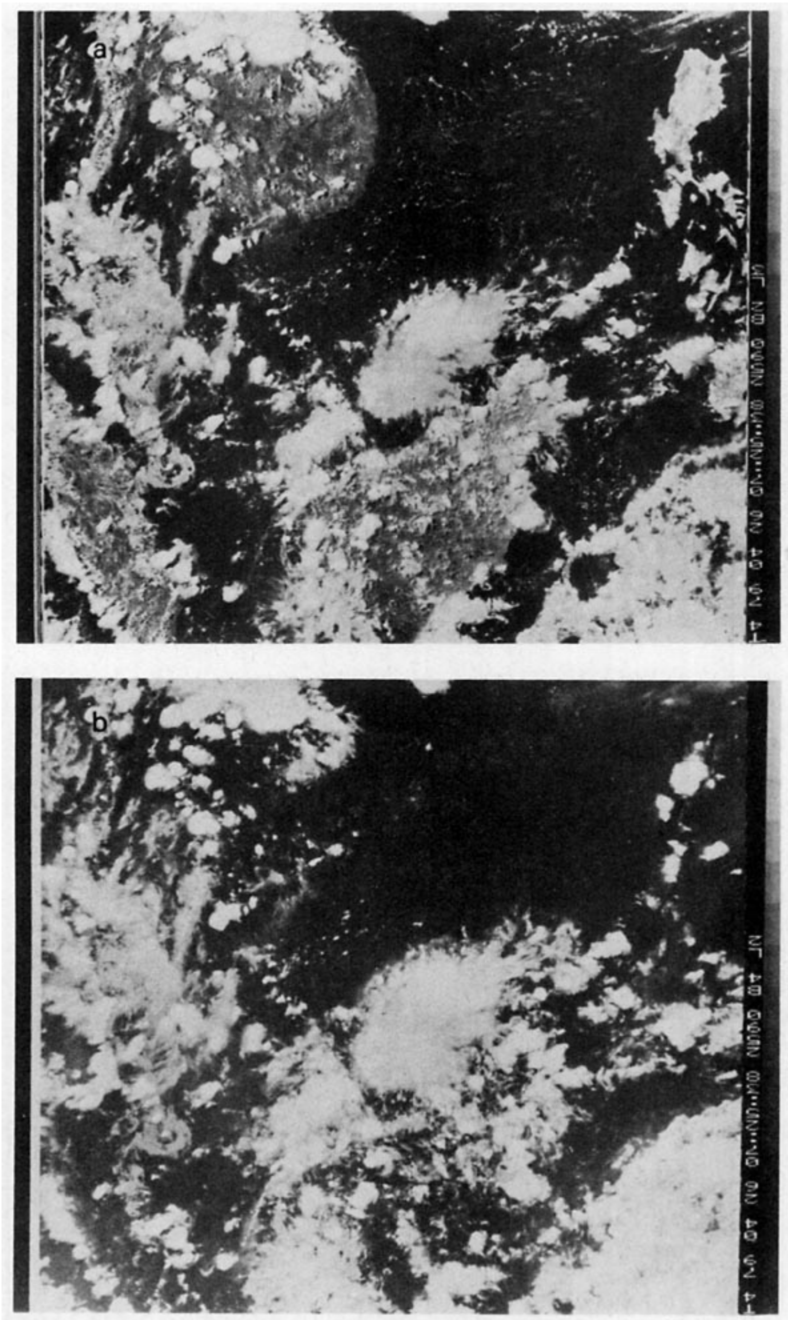

FIG. 2. Tiros N image observed through the (a) visible spectrum (b) 10 μm atmospheric window over the South China Sea. The clouds of interest appear at top center.

then the blackbody radiation within the band ($\Delta\lambda = \lambda_2 - \lambda_1$) can be approximated by

$$B(T_c) = \sigma T_c^4[S(\lambda_2, T_c) - S(\lambda_1, T_c)], \quad (10a)$$

$$B(T_s) = \sigma T_s^4[S(\lambda_2, T_s) - S(\lambda_1, T_s)], \quad (10b)$$

$$B(T_{sun}) = J_0 \cos\theta[S(\lambda_2, T_{sun}) - S(\lambda_1, T_{sun})], \quad (10c)$$

where

σ = Stefan's constant = 5.67×10^{-8} W m^{-2} K^{-4},

J_0 = solar constant = 1.367×10^3 W m^{-2}.

Evaluation of the blackbody radiation terms in (10) within the near infrared band from $\lambda_1 = 3.55$ μm to $\lambda_2 = 3.93$ μm presents some difficulty as ordinary Planck tables cannot provide such resolution. Following Goody (1964), and with $x = C_2/\lambda T$, $S(\lambda, T)$ can be approximated as

$$S(\lambda, T) = \begin{cases} x^3 e^{-x}/6.4939, & x \to \infty, \quad (11a) \\ 1 - 0.05134x^3, & x \to 0. \quad (11b) \end{cases}$$

At $\lambda = 3.55$ μm and $T = 5800$ and 300 K, x is equal to 0.7 and 14, respectively. These values are sufficiently close to zero and ∞ as to permit the use of (11a) and (11b) which, when compared with tabulated values, underestimate the blackbody radiation by about 20 and 0.5%, respectively. In view of the large uncertainties involved in the evaluation of α_c and α_s, such uncertainties can be tolerated.

There now remains the problem of determining the values of α_c and α_s. Unfortunately, we know of no relevant experimental investigations of spectral albedo of clouds and sea surface, we have to rely on theoretical calculations.

The albedo values of cloud (α_c) in the 3–4 μm transparancy windows were calculated by Feigelson (1964) for a water content of 0.2 g m^{-3} and different temperatures (T). Her values for the 3–4 μm case are tabulated in Table 2. These values agree quite well with those calculated by Bauer (1964) who obtained an albedo of 10.9% at 3.5 μm wavelength and of 15.7% at 4.3 μm.

The spectral albedo of a smooth sea can be calculated from the Fresnel formula (Kondratyev, 1969) for specular reflection from a water surface and indicates a steady decrease of albedo with increase in wavelength, an effect which is more pronounced at high angles of incidence. However, even at high angles of incidence the variation of the dependence of albedo on wavelength is quite low (Kondratyev, 1969), and can be considered to be practically independent of wavelength in the region of interest.

Albedo values over a wind-roughened water surface will be different from those which would be expected from a smooth water surface (Burt, 1954). Table 3 shows some of the values measured by Payne (1972). It can be observed that the albedo values decrease rapidly at first followed by a more gradual decrease as the solar altitude increases. This effect is well demonstrated by the calculations of Kondratyev and Ter-Markariantz (1953, 1956) and measurements of Sivkov (1952), Grishchenko (1959) and Nunez *et al.* (1972). There also is quantitative agreement between their data and that of Table 3.

Using these values of α_c and α_s, together with the Eqs. (3)–(11), G can be evaluated for cloud and sea surface elements on the satellite picture, thus determining the appearances of their relative shades.

TABLE 1. Empirical bidirectional function [Green (1980) for an azimuthal angle (ξ) of 270°].

ρ ϕ / θ	10°	30°	80°
20	0.318	0.315	0.309
50	0.272	0.275	0.329
80	0.209	0.236	0.491

TABLE 2. Albedo of a stratus cloud in the 3.7 μm atmospheric window.

α_c T (K) / λ (μm)	258	268
3	0.09	0.06
3.4	0.12	0.12
4	0.24	0.22

3. Results and discussion

In Fig. 1 the sea temperature in the area of interest is ~29°C (T_s = 302 K). Visible and 10 μm infrared images (Fig. 2) indicate that the "dark" clouds concerned are fair weather cumulus and the cloud-top temperatures are estimated to have a lower limit of about −5°C (T_c = 268 K). At the time when the image in Fig. 1 was taken the sun was overhead at ~75°E and as the area of interest is near 16°N, 115°E, θ, ϕ and ξ are estimated to be ~50, 30 and 270°, respectively.

From Table 1 the albedo of clouds at T_c = 268 K ranges from 0.12 at 3.4 μm to 0.22 at 4 μm. In the 3.7 μm window we take an average α_c value of 0.18. From Table 3 the albedo of the sea surface at a solar zenith angle of 50° is 0.44 and from Table 1 ρ(50, 270, 30) = 0.275. From (3) and (7) G can now be calculated as a function of L and it can be seen in Fig. 3 that the inequality $G > 1$ can be satisfied for both the limiting cases of a diffuse model (L = 0) and the empirical bidirectional model (L = 1).

The sensitivity of the dependence of G to the uncertainties in α_s and α_c is shown in Fig. 4 where it can be seen that within the range of uncertainties in α_s and α_c values, G attains a value > 1 provided that $\alpha_c > 0.14$ (i.e., a lower uncertainty limit of −20%).

TABLE 3. Albedo of sea surface (after Payne, 1972).

Solar altitude (deg)	Albedo of sea (α_s)
20	0.122
40	0.044
60	0.026

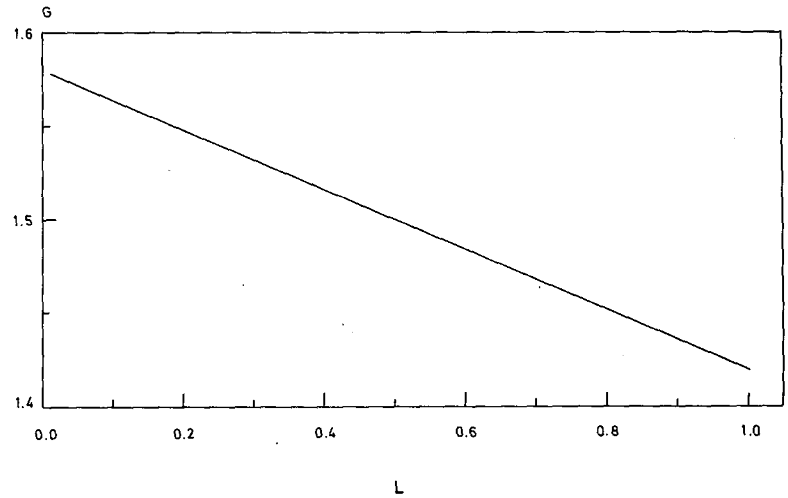

FIG. 3. Variation of G with model parameter L.

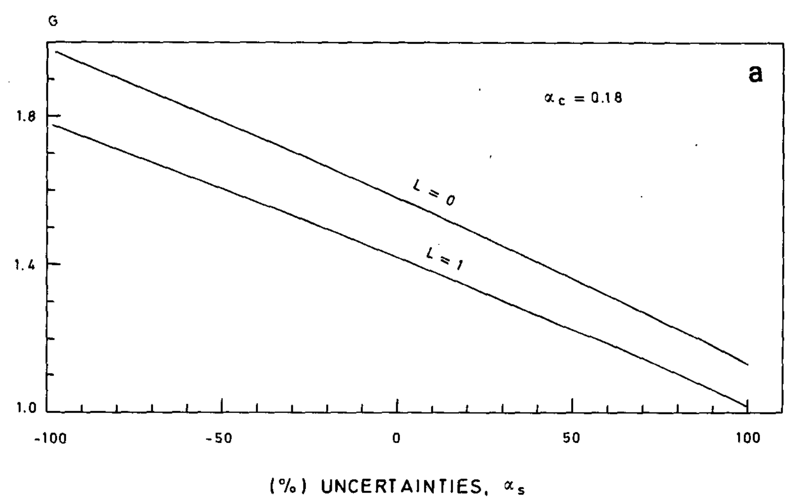

FIG. 4a. Dependence of G on α_s for an α_c of 0.18.

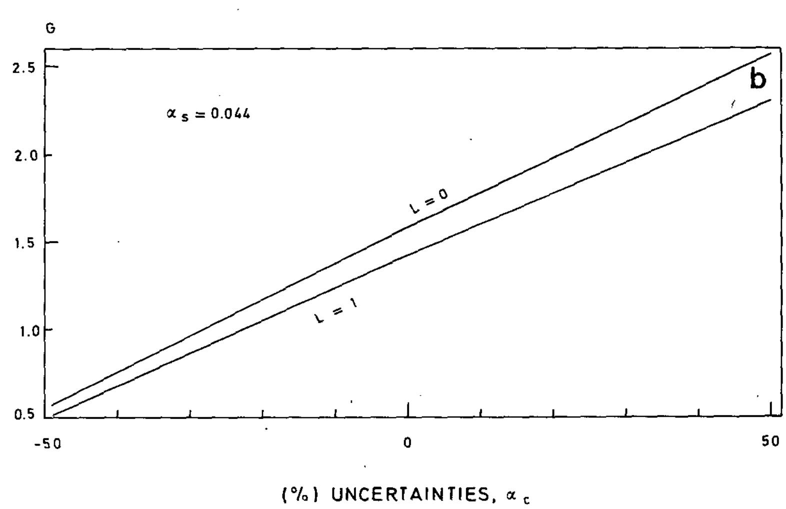

FIG. 4b. Dependence of G on α_c for an α_s value of 0.044.

The above calculations using the best estimates of the various parameters indicate that $G > 1$ for clouds having temperatures higher than 268 K; they therefore appear dark over a greyish sea in the area of interest. Clouds with lower temperatures will be whiter than the sea.

It is of interest to note that there exists a value of T_c such that $G = 1$. A cloud that meets this criteria would be indistinguishable from the sea. This equality can be used to estimate the albedo of clouds in the 3.7 μm window using (7). T_c and T_s can be estimated from simultaneous images in the 10 μm band to within 5°C. α_s can be considered as being independent of wavelength and can be obtained either from Fresnel's relationship for smooth sea or from Payne's (1972) measurements. These values of T_c, T_s and α_s can then be used in (7) to estimate the cloud albedo α_c, by either using a diffuse model or the empirical bidirectional reflectance model.

REFERENCES

Bauer, E., 1964: Scattering of infrared radiation from clouds. *Appl. Opt.*, **3,** 197–202.

Burt, W. V., 1954: Albedo over wind-roughened water. *J. Appl. Meteor.*, **11,** 283–290.

Feigelson, Ye, M., 1964: *Radiation Processes in Stratus Clouds*. Nauka, 245 pp.

Goody, R. M., 1964: *Atmospheric Radiation*, Clarendon Press. 403 pp.

Grishchenko, D. L., 1959: The dependence of albedo of the sea on the altitude of the sun and disturbance of the sea surface. *Tr. Glav. Geofis. Observ.*, **80,** 32–38.

Green, R. N., 1980: The effect of directional radiation models on the interpretation of earth radiation budget measurement. *J. Atmos. Sci.*, **37,** 2298–2313.

Kondratyev, K. Ya, 1969: *International Geophysics Series*. Vol. 12, Academic Press.

——, and N. E. Ter-Markariantz, 1953: Albedo of the rough sea. *Gidrometeor.*, **6,** No. 8, 45–51.

——, and ——, N. E. Ter-Markariantz, 1956: On the reflection of radiation by the sea. *Proc. Leningrad University, Ser. Phys.*, No. 9, 210 pp.

Nunez, M., J. A. Davis and P. J. Robinson, 1972: Surface albedo at a tower site in Lake Ontario. *Bound.-Layer Meteor.*, **3,** 77–86.

Payne, R. E., 1972: Albedo of sea surface. *J. Atmos. Sci.*, **29,** 959–970.

Sivkov, S. I., 1952: The geographical distribution of effective albedo of water surface. *Izv. Vses. Geogr. Obshch.*, **84,** 200–201.